

Received 6 December 2023, accepted 30 December 2023, date of publication 8 January 2024,
date of current version 17 January 2024.

Digital Object Identifier 10.1109/ACCESS.2024.3351210

RESEARCH ARTICLE

Artificial Marker to Predict (Banganapalle) Mango Fruit Size at Multi-Targets of an Image Using Semantic Segmentation

DEVENDER NAYAK NENAVATH¹ AND BOOMINATHAN PERUMAL¹, (Member, IEEE)

School of Computer Science and Engineering (SCOPE), Vellore Institute of Technology, Vellore, Tamil Nadu 632014, India

Corresponding author: Boominathan Perumal (boominathan.p@vit.ac.in)

This work was supported by the Vellore Institute of Technology (VIT), Vellore, India.

ABSTRACT Getting the size of any fruit on a tree is not an easy task especially mango fruit, because of its irregular shape, it is not easy to model with its shape. The size of the fruit is expected in length and width. Objective: Horticulture farmers need to engage in extra activities to obtain better yields, such as trying to know the fruit shape and size at the time of maturity, or before plucking the fruits from the tree, which will help farmers obtain as per their predicted price while selling the fruits to the market. Methods: Researchers applied a deep learning model called YOLOv7, semantic segmentation, to obtain fruit size using an aruco marker and proposed a technique to help farmers as detect markers and the fruits in images and predict the size of the fruit at multiple targets. A custom dataset was created by collecting mango fruit frames from an on-tree-mango-360° recorded video. After training and validating the model, its performance is tested using a test dataset. Results: The contributions of this study are as follows: The researcher developed a procedure to obtain mango size from an image. The researcher implemented and tested a model to detect mangoes in different challenging situations using YOLOv7 with semantic segmentation. This model achieves excellent results for fruit size estimation. The training and testing results of YOLOv7-SS-AM show that the Aruco marker-based model is superior to manual size prediction, with good accuracy.

INDEX TERMS ArUco, aruco-marker, semantic-segmentation, shape, YOLOv7.

I. INTRODUCTION

In recent years, estimating the fruit size [24] on trees using computer vision has become very difficult. In orchards, on-tree mango fruit volume [10] and size estimation are important for managing early season mango crop loads and harvesting. If the farmer is well known about the fruit size, then the farmer can expect an accurate outcome of the mango fruit yield in the mid-season, which will allow him to plan for labor, the need for the number of fruit bins, and the required storage space at the time of harvest.

Reference [8] a synthetic square marker, aruco, was used to detect mango fruit size. The Aruco marker is an artificial augmented reality marker that also has a library for OpenCV that can be used in computer vision for size estimation.

The associate editor coordinating the review of this manuscript and approving it for publication was Senthil Kumar¹.

To obtain the localize the fruit on the tree, the image segmentation concept is used, [22] Image segmentation is used in image processing and computer vision to understand the scene by partitioning the image into multiple segments as individual labels for instance segmentation [7] or semantic labels for semantic segmentation [16] of the same objects to separate the fruit, leaves, and branches. Another segmentation method is called panoptic, [20] which segment both the object of the image and the remaining object within a single-output image. The major benefit of image segmentation is that it improves computational efficiency and accuracy by eliminating background noise. Image segmentation can be more general than object detection and recognition and can provide theoretical and deep insights into the work and limitations of visual systems [15]. The three major types of image segmentation techniques are instance, semantic, and panoptic segmentation. We can visually observe the differences between the three segmentations in Figure 1.

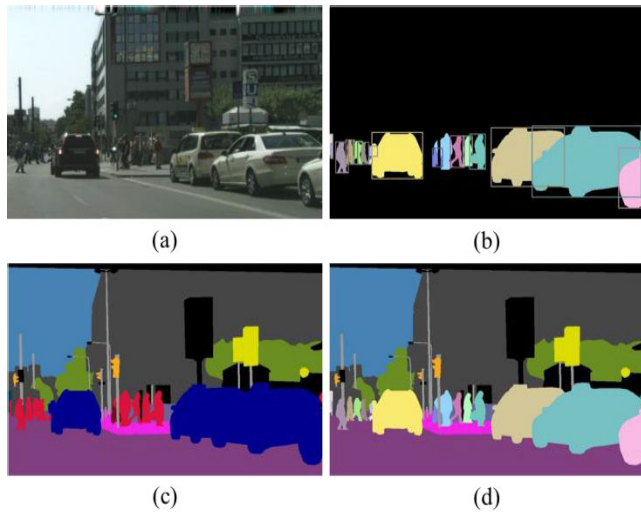


FIGURE 1. (a). Original image of cars at junction, (b). Instance segmentation, (c). Semantic segmentation, (d). Panoptic segmentation. The figure is partially borrowed from [19].

Compared with instance segmentation, semantic segmentation is very useful in horticulture and agriculture, the purpose of which is its characteristic. Semantic segmentation, also known as scene labeling, refers to the assignment process of assigning the same category label to each pixel of an image [36]. Instance segmentation labels different colors for different objects, whereas semantic segmentation labels the same colors for a group of objects. In this study, the researchers focused on measuring the size of fruits. Therefore, using semantic segmentation, it is possible for a researcher to obtain all the fruits in the image to measure their size.

A. CONTRIBUTIONS

This study aims to determine the size and shape of mangoes by computer vision using a deep learning algorithm. When the camera, mango, and background are in motion, if the farmer needs the size of the fruit on the tree, the farmer must make a round video capture of 360° of the trees. The camera, fruit, and background are in motion, which means that the camera, foreground, and background are not fixed, and that all three are in motion. Detecting and obtaining the size of a mango on a tree is very difficult to measure the size. Our aim was to obtain the size of multiple mango fruits using computer vision with high accuracy using deep learning models.

Combining YOLOv7 for object detection and ArUco markers for size measurement is a powerful approach for accurately detecting objects in an image and measuring their size. By combining YOLOv7 for object detection with ArUco markers for size measurement, we can achieve accurate object detection and precise size measurements in a single pipeline. This approach is particularly useful for measuring objects of various sizes in real-world scenarios.

Fruit detection on trees and fruit size measurements in the laboratory are available, but fruit size measurement on trees

is not, which will provide farmer income prediction where the farmers are very grateful. With the proposed method, horticultural farmers can predict fruit weight based on fruit size using computer vision, which will affect their future. There are various possible methods available; however, no method is available based on fruit size, such as height and width, no method is available. If this type of model is available, farmers can easily predict fruit size and estimate fruit size to predict fruit weight after building an application based on this model.

The use of ArUco markers and YOLOv7 to measure the size of an object is an interesting approach to solving various problems related to object measurement and tracking. Some potential applications and problems that can be addressed using this method are as follows: in agriculture, the farmer can attach the marker to plants, and using YOLOv7, they can detect plant dimensions that can assist in monitoring plant growth rates and identifying potential issues. It can solve architectural design measurement problems by placing markers in architectural models, Inventory Management in Warehouses using these ArUco markers on items or shelves, and YOLOv7 to detect and measure the size of items. This can assist in efficiently maintaining the inventory tracking. In medical imaging [30], ArUco markers are attached to instruments or used as reference points in medical imaging and then measure sizes. This information can be used for medical diagnostics and treatment planning.

II. RELATED WORK

Passive markers are used to satisfy the requirements of a multitarget fruit size for the same object in an image, some passive markers are used [37]. These markers are inexpensive and easy to use to do the work for computer vision-based models. A few of these are QR codes and augmented reality markers such as ARTag [17] and Artoolkit [18]. Another marker, Aruco, uses the same approach as ARTag and Artoolkit. It was observed that The Aruco marker had a small false-positive rate in cases of occlusion.

Based on [34], their work was extended from the detection of fruit to determining the fruit size, and found the fruit size based on the original image input by cascade fruit detection using HOG features [35], then identified fruit by cascade fruit detection, to remove the background Otsu's method and color thresholding methods, filtered the stalk, and performed a depth registration. Then, the fruit size was calculated from the bounding box side length with a single fruit bounding box and achieved 100% precision using the ellipse fitting method and 81.1% precision using % the cascade detection method.

Reference [23] developed a machine vision system using synchronized stereo cameras on an LED strobe to obtain the size from on-tree fruit images with high accuracy. Faster R-CNN and Mask R-CNN models were used, and to handle some fruit occlusions, the convolutional network was trained on extrapolating fruit boundaries, compared to the caliper-measured fruit diameter [23], which was a stronger predictor.

Reference [3] observed how much the (*Mangifera indica*) that increased in size from day to day was estimated in the form of height, width, and thickness. The linear measurements of the weekly increase in fruit mass with the linear regression model by an $R^2 > 0.88$ and the slope is 19.6 ± 7.1 g/week, depending on the season, site, and cultivar. The fruit mass in the field was measured at 400–450 growing degree days (GDD) units before harvesting GDD and one week later.

Reference [13] implemented a CNN model named amodel instance segmentation which will do segmentation better than the previous model named model segmentation which limits the visible region of fruits whereas in amodel segmentation it will predict the fruits occluded region with the fruits visible region which will give us the complete shape of the fruit and the predicted visible diameter was greater than 60% of accuracy.

III. MATERIALS AND METHODS

Determining the object size using computer camera vision is not an easy task. Manual sizing of objects will take more time to complete, but using some deep learning models for object size will give some fast results, save time, and improve accuracy. We incorporated the use of image processing concepts with a deep learning model to determine the object size in a bounding box format for the length and width of the object.

It is easy to find an object without multiple backgrounds. However, if multiple objects have multiple backgrounds, it is not an easy task. To determine object size using these features, Semantic segmentation was used to train objects to determine their size using these features. This problem is prevalent in agricultural horticulture. It is difficult for farmers to determine the fruit size of trees. The researcher contributed to this work by obtaining the fruit size on the tree using YOLOv7, semantic segmentation, artificial markers, and background subtraction to ease their work.

The main goal of this study was to measure mangoes of different sizes on a tree using YOLOv7 and Aruco markers. Mango detection was performed using YOLOv7 on tree mangoes, and the YOLOv7 algorithm provided bounding boxes around the mangoes. After YOLOv7 detects mangoes, the researcher uses semantic segmentation for background removal from the image and provides all fruits that were present in that particular image. Aruco marker detection was used to identify whether any image contained an aruco marker, and a computer vision library such as OpenCV was used to detect and recognize aruco markers within the bounding boxes of detected objects [26]. Once the researcher detects the aruco markers within the object scene, they can measure their size by using the known physical size of the markers. Aruco markers are designed with known dimensions; thus, the scale factor can be calculated by comparing the size of the detected markers in pixels with their known sizes, the scale factor can be calculated. With the scale factor determined from the aruco markers, this scale can be applied to the dimensions of the objects detected by YOLOv7.

This allowed us to convert the pixel measurements of the objects into real-world physical measurements for precise measurements. Finally, the size of the detected objects in the desired units was measured in centimeters based on the Aruco marker scale. Therefore, in this pipeline, the researcher observed that the aruco marker cannot measure fruit size if the scene contains multiple backgrounds, as the fruit is on the tree. Therefore, the fruit will be visible, including the leaf and branch. For this purpose, the researcher used semantic segmentation in this pipeline to remove multiple backgrounds from the scene, and only the fruits were in the visible mode. The aruco marker measurement procedure then enters this process. Finally, the fruit size was visible on the scene.

A. YOLOV7 ALGORITHM FOR ON TREE MANGO DETECTION

The YOLOv7 algorithm was used, Figure 2 Compared to known one-stage object detectors YOLOv7 algorithm surpasses in both accuracy and speed range from 5 FPS to 160 FPS, with the highest average precision of 56.8%, and compared to the recent YOLOv6 average precision of 43.1% YOLOv7 is 13.7% higher [33]. YOLOv7 is the best choice for high-resolution inference, albeit at a lower speed.

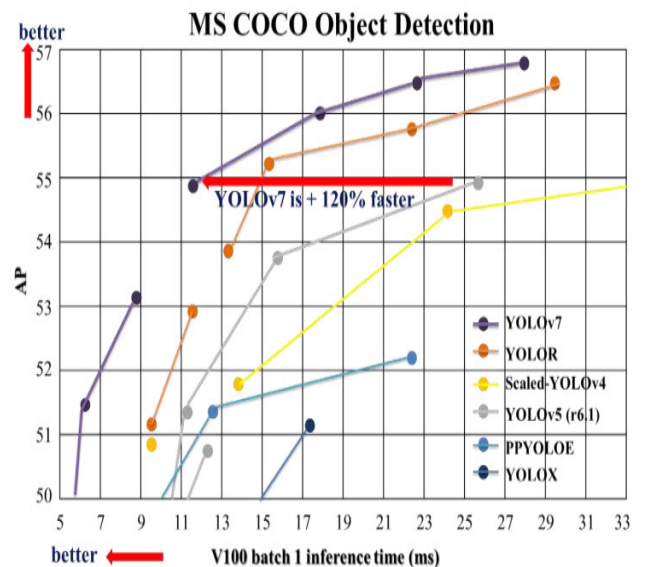


FIGURE 2. Comparison with other object detectors with the YOLOv7 object detector model.

On-tree mango detection was performed using the YOLOv7 algorithm, which created its own dataset. The dataset was trained using YOLOv7 for 100 epochs Figure 3. At the time of testing, this algorithm performed well on the test images, where the researcher split the dataset in a ratio of 80% for training and 20% for testing.

Some advantages of using YOLOv7 are its real-time object detection capabilities. YOLOv7 can detect a wide range of objects, and is not limited to specific markers [21]. YOLOv7 can handle dynamic scenes with moving objects

and changing background. In addition, the accuracy of YOLO may not match the precision of aruco markers for size measurements in controlled environments.

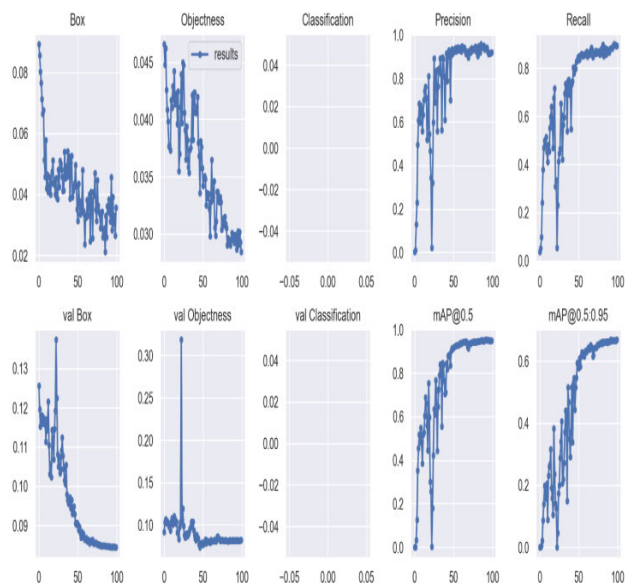


FIGURE 3. On-tree mango fruit training results using YOLOv7 on a custom dataset. Number of epochs on the x-axis, and confidences on the y-axis.

B. SEMANTIC SEGMENTATION

The aruco marker can identify a mango object; however, when multiple backgrounds are present, it cannot be detected without removing them. Therefore, a segmentation method was used that partitions an image into different sub-key parts for simplification to change the representation in an image and make it meaningful for analysis. Using an aruco marker as a reference, the entire scene of an image can be detected, including the fruits, leaves, and branches. If the fruits are on any single background, such as white/black, only the fruit is visible, and the aruco marker can only detect the fruit without any error. The segmentation concept was used to overcome these background objects and to hide and detect only fruits with multiple backgrounds that were removed by semantic segmentation. Segmentation methods are still widely used in computer vision and image processing for object detection and recognition for several reasons such as versatility, scalability, and noncontact [15]. Based on the main components of recent semantic segmentation methods, semantic segmentation can be divided into three categories: region-based, FCN-based, and weakly supervised semantic segmentation. Region-based semantic segmentation follows segmentation using a recognition pipeline that extracts and describes freeform regions from an image followed by region-based classification. Region-based predictions were transformed into pixel predictions at the test time by labeling a pixel according to the highest-scoring region [6]. In FCN-based semantic segmentation, pixel-to-pixel mapping is performed pixel-to-pixel without extracting the region proposals [28],

and weakly supervised semantic segmentation is used to overcome a large number of images with pixel-wise segmentation masks, where manually annotating masks are performed, which is time-consuming and very expensive [15].

1) SEMANTIC SEGMENTATION LABELING TOOL

Fiji [27] used modern software that combines powerful libraries to enable the rapid prototyping of image-processing algorithms with a broad range of scripting languages. It is a modern software that uses the open-source software ImageJ, which focuses on biological image analyses. Fiji contains plugins that are helpful for labeling. The researcher used Labkit. LabKit is a labeling and segmentation plugin for large image datasets that provides pixel classification for automatic segmentation [4].

C. ARUCO MARKER PREPARATION

Aruco markers are specially designed square markers with a unique pattern of black and white squares [14]. Each Aruco marker is manufactured with known physical dimensions. Using computer vision techniques, aruco markers were detected and located in images [5]. Popular computer vision libraries such as OpenCV provide tools for recognizing and extracting aruco marker positions and orientations. Once an aruco marker is detected in an image, its known physical dimensions can be used as reference. By measuring the size of the marker in pixels within the image, a scale factor that relates pixels to real-world units such as centimeters or inches can be obtained [9]. With the determined scale factor, we can now measure the sizes of other objects in the image. When an object of interest is detected, its dimensions can be calculated in real-world units by multiplying the number of pixels with an established scale factor. Aruco markers are designed to be highly detectable and have well-defined corners and edges, which make their detection and size measurement relatively accurate. aruco markers can be used to measure the sizes of multiple objects within the same image, even if the objects have varying sizes and orientations. Unlike physical measurements that require contact with an object, aruco marker-based measurements are non-contact, which can be advantageous in scenarios where contact is not feasible or could affect the integrity of the object. Aruco markers serve as reliable references for size measurements within an image, enabling accurate and consistent measurement of object dimensions. They are particularly valuable in computer vision applications, where precise size information is required for tasks, such as quality control, object recognition, and dimensional analysis.

The aruco marker was developed for camera pose estimation [12]; however, the researcher used this artificial marker for fruit size estimation. There are [29] 4×4 , 5×5 , 6×6 , and 7×7 markers, and the available total number of possible ids is 50, 100, 250, and 1000, respectively. The aruco markers was downloaded from its genuine website based on the requirements of the user shown in Figure 4, printout it, and paste it on a sheet where we are going to use it for size

estimation [31]. There is a possibility to find the marker ID from the original marker, as shown in Figure 5, which follows the Huffman coding [25] procedure.

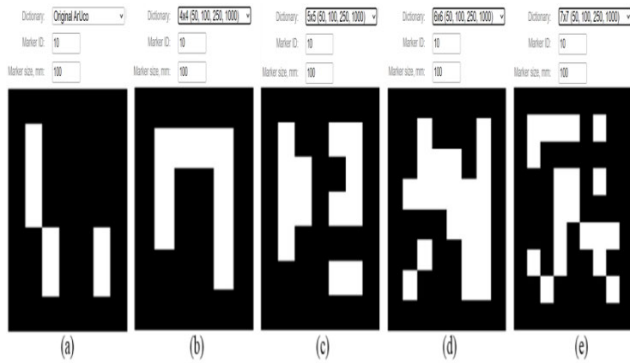


FIGURE 4. Different types of markers were available based on different matrix sizes. (a). original ArUco marker, (b) 4 × 4 with marker ID: 10, (c) 5 × 5 with marker ID: 10, (d) 6 × 6 with marker ID: 10, (e) 7 × 7 with marker ID: 10.

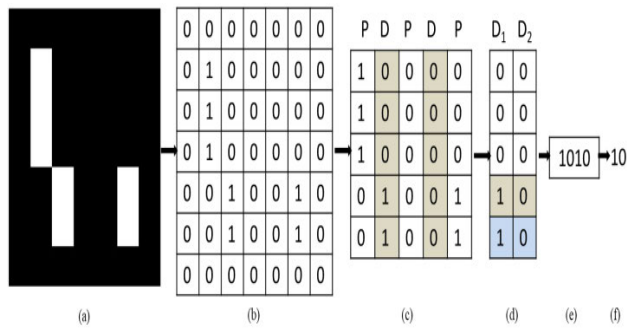


FIGURE 5. Based on the original marker, the ID of the particular marker was found, (a) Original ArUco marker, (b) Converted in binaries as 0 for black color, and 1 for white color, (c) First, Third, and Fifth bits as parity bits, and Second and Fourth bits as data bits, (d) Selected data bits, (e) 000001010 as 1010 Final binary digits of the marker, (f) Founded ArUco marker ID.

Some advantages of using aruco markers for fruit size measurement include their high accuracy as they provide high-precision size measurements because of their known physical dimensions. Finally, aruco markers offer consistent measurements that render them suitable for quality control and repeated tasks. In additionally, aruco markers require physical markers to be attached to objects, which may not always be practical. They are best suited for relatively static scenes, because marker detection may be affected by object motion or occlusion. Marker detection is challenging in complex and cluttered environments.

D. MEASURE MANGO FRUIT SIZE USING THE DETECTED ARUCO

Based on the aruco marker detection [31], it is possible to find the centroid of the marker Refer to “(1),” where (a_1, b_1) , (a_2, b_2) , (a_3, b_3) , and (a_4, b_4) are the corners of the marker, from the corners (a_c, b_c) are the spatial coordinates of the Centre of the marker Figure 6, and these are evaluated

Refer to “(1),” (a_r, b_r) are the coordinates of r^{th} vertex, and \vec{G} , is the spatial calibration vector which will use to convert the image from pixels units to SI units as the ratio of physical marker side length d_{SI} and the side length vector of pixels \vec{d}_{px} , along the x-axis and y-axis as shown Refer to “(2),”

$$C = (a_c, b_c) = \vec{G} \cdot \left(\frac{1}{4} \sum_{r=1}^4 |a_r|, \frac{1}{4} \sum_{r=1}^4 |b_r| \right) \quad (1)$$

$$\vec{G} = d_{SI} / \vec{d}_{px} \quad (2)$$

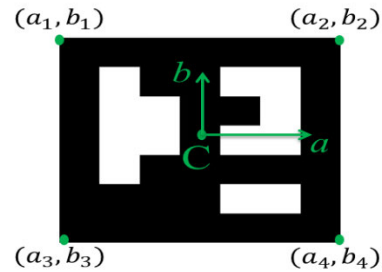


FIGURE 6. Example of ArUco marker ID: 10 from the original marker dictionary.

The researcher expected fruit size to be in the form of height and width. Based on the above methods, it is possible to obtain the size in terms of the height and width. From the formula below, if there is a possibility of a three-dimensional value of the fruit, it will be useful; however, in this study, the researcher directly obtained the height and width of the fruit in two dimensions.

Reference [34] Fruit size $S = w \times (\frac{b+1}{2})^2$, where $(\frac{b+1}{2})^2$ is the height of the fruit and w is the width of the fruit. Here, b is the breadth and l is the length.

E. WORK FLOW DIAGRAM OF YOLOv7-SS-AM

The researcher followed the model below for fruit size estimation, developed a new model, and obtained on-tree fruit sizes with better accuracy than other models. The steps are shown in the workflow diagram in Figure 7.

- Step 1: The Banganapalle mango dataset was created in the morning lighting conditions between 06:00 AM and 08:00 AM, where the chances of obtaining a fruit shadow are very low with 80% and 20% of the training and testing ratios of 80 and 20, respectively, at the first step for on-tree mango detection.
- Step 2: Input image for finding the mango fruit size
- Step 3: Detect mangoes using YOLOv7, where the fruits are available in a given input image.
- Step 4: Analyze the dataset and detect banganapalle mangoes in the input image.
- Step 5: Use the Fiji LabKit tool and perform semantic segmentation to ensure the successful training of the image is successfully trained.
- Step 6: Perform background removal on the segmented image, and remove the background image.
- Step 7: Use ArUco marker with the background removed image for size estimation.

- Step 8: Store the estimated fruit size in the results for future reference.

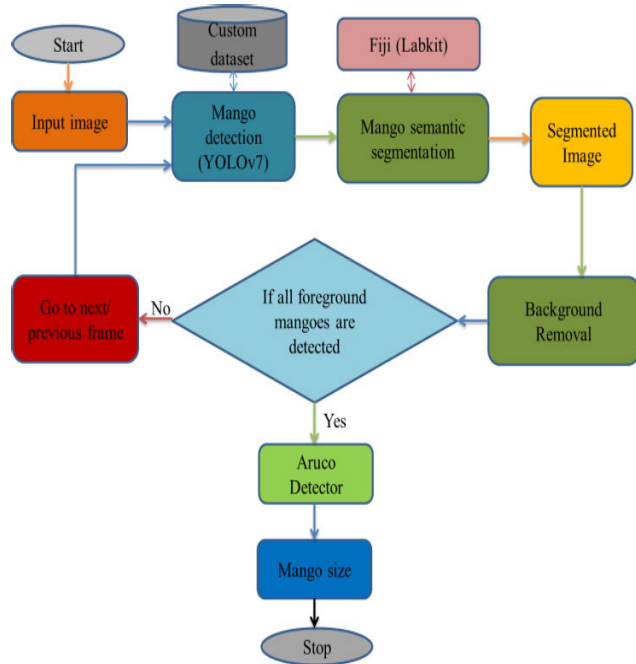


FIGURE 7. Workflow from input image to mango size prediction with YOLOv7-SS-AM.

F. DATA PRE-PROCESSING

At the mature stage of fruit on the tree, a 360° video around the tree was captured in the morning between 06:00 AM and 08:00 AM in Telangana State, India, during the summer. The video was captured using an iQOO Z3 5G mobile phone with 1080 × 1920 pixels at 30fps of speed. The video was split into frames and 224 image frames were selected to prepare the dataset using the Labellmg tool [32], which is useful for image annotation in image processing and classification. Subsequently, all images were annotated and divided at a ratio of 80:20 for training and testing purposes. At 80:20, 179 image frames were used for training and 45 image frames were used for testing and validation. Basic filters, such as Gaussian blur and the Laplacian of Gaussian for each sigma, were used at the time of image annotation.

IV. RESULTS

A. OCCLUDED FRUITS DATA

After all the procedures, the researcher developed a model and obtained the results for fruits of different sizes, as shown in Figure 8. This YOLOv7-SS-AM model worked very accurately, but in the case of occluded fruits, it did not perform well and had some errors when the fruits occluded each other. This model showed it as a fruit and its size as a single fruit size, and provided approximate accuracy for occluded fruits.

$$Accuracy = \frac{\text{Number of size estimated fruit}}{\text{Number of detected fruits in an image}} \quad (3)$$

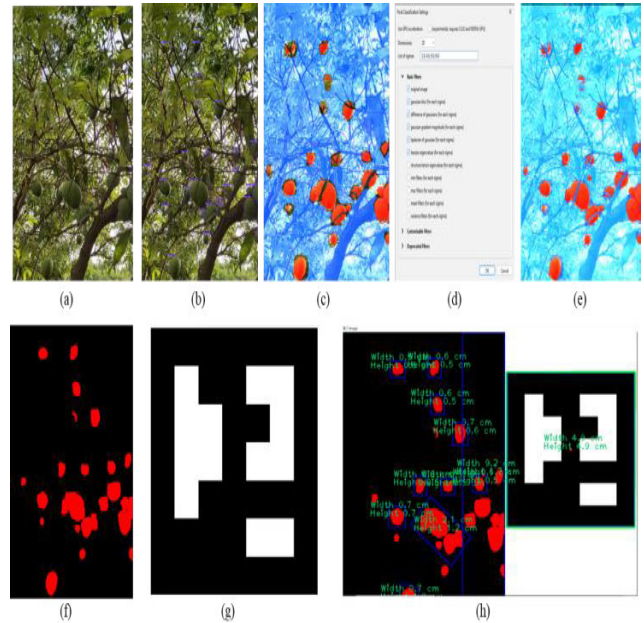


FIGURE 8. Method procedure to get the size of the fruit in a bounding box format: (a). Original image of Frame10, (b). bounding box on all detected images using YOLOv7, (c). Manual labeling using Labkit for pixel classification. (d). filters used to train the image, (e). After training the image, the foreground and background separation using semantic segmentation classifier, (f). Background removed and foreground displayed (g). 5 × 5 size aruco marker which is used for fruit size estimation, (h). Size of the fruit and the aruco marker with the expected result.

At the time of a single background, if there is only one fruit in an image scene then the detection and the size measurement accuracy of the fruit is more than 99%, if the image with a single background contains multiple fruits without any overlapping also provides more than 96.7% accuracy with Refer to “(3),” if the fruit is on-tree overlapped then there are two ways to get the accuracy. One is the fruit that overlaps with a leaf or branch and the other is the fruit occluded with another fruit. In the first mode, the fruit overlaps with the leaf or branch, and the accuracy of fruit detection is similar to that of nonoccluded fruits. According to [13], the occluded part of the fruit was considered and full-length fruit was measured, whereas in the second mode, the fruit occluded with another fruit, the accuracy will differ as fruit overlap increases, and the accuracy will decrease at the occluded fruit only at 84%. Based on the results, the occluded detection accuracy was good, but the size accuracy was the sum of the occluded fruits in an image. Therefore, the YOLOv7-SS-AM model is fully applicable and useful for non-occluded voluntarily visible fruits in tree mango size measurements, and 84% is applicable for on-tree overlapped mango fruits with other fruits, excluding occluded leaves or branches in tree measurements, as shown in Figure 9.

Analyzing and demonstrating the robustness and universality of the proposed method for object size measurement using ArUco markers and YOLOv7 for detection is an important step in validating the effectiveness of our approach. Figure 10 shows the validation of the used and predicted data for

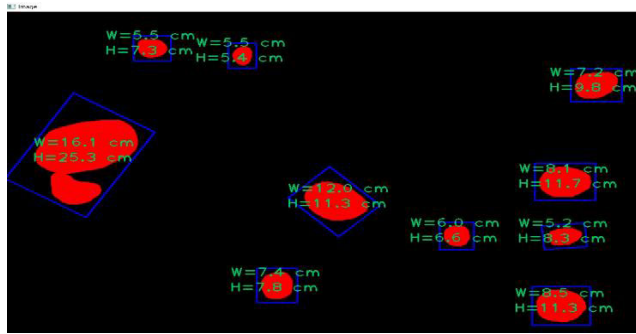


FIGURE 9. Ocluded fruit detection and size estimation.

overlapping fruits on tree mangoes for the size estimation. The actual size was measured manually and stored for validation, the predicted size was measured using the model, and a close comparative result was obtained.

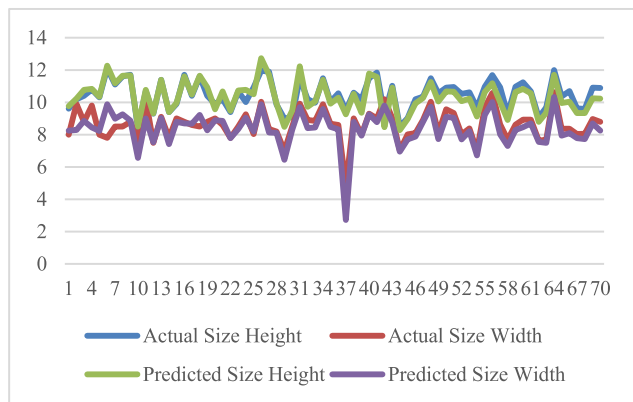


FIGURE 10. Overlapped fruit's actual size and predicted size in the form of height and width.

B. NON-OCCLUDED FRUITS DATA

Based on the YOLOv7-SS-AM model, the researcher determined the size of the fruit where the fruits were not occluded and were clearly visible was determined. Following the same model, the following steps were followed: The researcher used mango fruits tied up with a thread and hooked them up on the wall with an aruco marker at a distance of 125 cm between the fruits and the camera. Video capture and images for future work. The researcher used images containing six different-sized mangoes and the aruco marker, which was 5 × 5 in size with marker ID 10 and assumed a size of 5 × 5. The resultant values are displayed in Figure 11, and the size of the aruco marker is predicted based on its perimeter.

Start the procedure for size estimation of mangoes as tree fruits. The steps described below were followed, based on the researcher-developed model.

- Step 1: Artificially prepared on tree image as input.
- Step 2: Detect fruit using the YOLOv7 algorithm.
- Step 3: A semantic segmentation tool was used to separate the background and foreground of the image.
- Step 4: Apply the background removal concept to the segmented image.

- Step 5: Remove the background from the image.
- Step 6: Focus on the foreground image for size prediction using the Aruco marker.
- Step 7: The Aruco marker displays the estimated size of the fruit as well as the marker width and height.

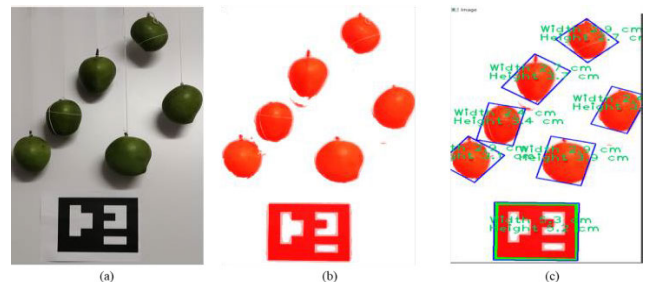


FIGURE 11. Result of the given input image using the proposed method, when there is no multiple background. (a). on tree mango input, (b). Background removal, (c). Mango size as bounding box with height and width.

However, in real-time, the sizes of the experimental aruco markers were differed. Therefore, the actual size of each fruit is given in Table 1, in which case the marker size was not 5 × 5 but was changed at the time of laboratory experimentation for clear visibility to 16 × 16. Based on the visible size of the marker, the perimeter also changed, and the fruit size was predicted clearly, as shown in Figure 12, with the actual fruit size and the predicted size for comparison.

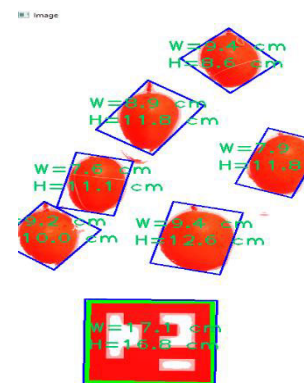


FIGURE 12. Predicted fruit size with aruco marker's perimeter as reference.

According to the data which was used for fruit size the researcher used some images, based on these images the researcher observed the fruit detection accuracy for size estimation at occlusion is 84% based on Refer to “(3),” using aruco marker as reference model with semantic segmentation on YOLOv7 detected images, and the researcher observed Precision is 91%, Recall is 89%, and the F1-Score is 90%. In contrast, for non-occluded mango fruit, Figure 13 the average accuracies of the measured height and width was 96.7%.

By observing Figure 9 of the image that was taken as an on-tree orchard image frame for overlapping work, in that the non-overlapping image part is there to imagine the accuracy

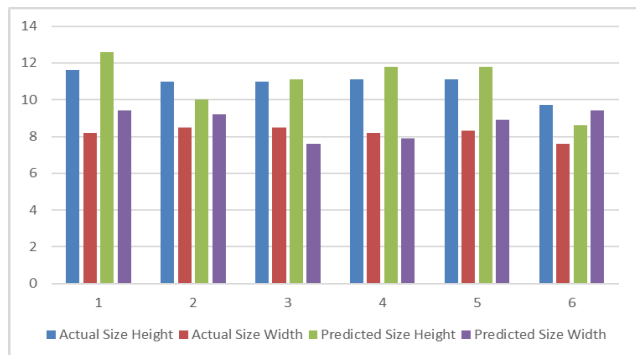


FIGURE 13. Non-overlapped On-tree mango fruit actual size and predicted size.

TABLE 1. Actual fruit size and the predicted size of the mango fruits.

Aruco Marker Size		Fruit Measurement			
Actual	Predicted	Actual Size		Predicted Size	
		Height	Width	Height	Width
$h \times w$ is	$h \times w$ is	11.6	8.2	12.6	9.4
16.0 cm ×	16.8 cm ×	11.0	8.5	10.0	9.2
16.4 cm	17.1 cm	11.0	8.5	11.1	7.6
		11.1	8.2	11.8	7.9
		11.1	8.3	11.8	8.9
		9.7	7.6	8.6	9.4

part of the fruit for on-orchard fruit size estimation, we can say that by following this model, it is good at non-overlapping the tree fruits of orchards.

V. DISCUSSIONS AND FUTURE WORK

A. DISCUSSIONS

Many image enhancement methods are available for image improvement in image processing; however, we did not improve image quality or brightness. Thus, researchers need to make only the fruits visible. For this, the researcher used background removal on an image, where they observed that only one fruit in the image was visible and the remaining fruits were not Figure 16. Although ArUco markers can be used in scenes with multiple backgrounds, their reliability depends on various factors including lighting, marker size, marker orientation, and background complexity. In complex and cluttered scenes, marker detection may become less robust, and alternative methods such as object detection and segmentation may be more suitable for identifying and tracking objects. Therefore, the semantic segmentation technique of image processing was used to segment the fruit into one class and the leftover part of the image into another class. They then applied background removal, removed the leftover class segment from the scene, and observed that all fruits in the images were visible in the image scene. There is a concept called image matting for image enhancement, which is similar to semantic segmentation. Semantic segmentation and image matting are two different computer vision tasks, although both involve the separation of objects from their backgrounds.

1) IMAGE MATTING V/S SEMANTIC SEGMENTATION

a: IMAGE MATTING

[11] Image matting focuses on creating a fine-grained pixel-level separation between the foreground object and background. It estimates the transparency or alpha value of each pixel, indicating the extent to which the pixel belongs to the foreground or the background. The output of image matting includes an alpha matte, which represents the transparency of each pixel. Along with the matte, you often obtain foreground and background color information are often obtained, allowing for high-quality compositing with new backgrounds. Image matting is employed in applications such as image and video compositing, virtual reality, and any scenario in which precise separation between an object and its background is required. Image matting is a more complex task because it requires estimating the alpha matte, which can vary smoothly across the object boundaries. This often involves solving an optimization problem and may require user interaction to obtain precise results. Image matting typically requires a dataset with alpha mattes, which can be challenging and time-consuming to obtain because they represent fine-grained object-background separation.

b: SEMANTIC SEGMENTATION

The goal of the SS is to classify each pixel in an image into a specific object class or category. It provides a pixel-wise label for each region, without considering the precise boundaries of the object. The output of semantic segmentation is a segmented image where each pixel is labeled with a class (e.g., “mango”, “tree”, “leaf”, “branch”). It does not provide information about object boundaries or transparency. Semantic segmentation is useful for tasks, such as scene understanding, object recognition, and image classification. It is commonly used to label regions of interest without requiring precise object boundaries. Semantic segmentation is a simpler task than image matting because it classifies pixels into predefined categories, often with the help of convolutional neural networks (CNNs). Semantic segmentation can be trained on datasets with image-label pairs, where each pixel is labeled with a class. This requires a less-detailed ground truth.

Compared with semantic segmentation and image matting, both involve segmenting objects from the background; they serve different purposes and have distinct outputs. Semantic segmentation classifies pixels into predefined categories, whereas image matting provides a fine-grained alpha matte to precisely separate objects from the background for tasks, such as compositing and visual effects.

The specific contribution is that YOLOv7 is markerless and does not require physical markers but may not provide the same level of precision for size measurements. Aruco markers are suitable for high-precision size measurements in controlled environments, whereas YOLOv7 excels in real-time and markerless object detection across various

dynamic and uncontrolled domains. The choice between these two methods depends on the specific requirements and constraints of their application.

2) ADAPTING PROPOSED MODEL

The combination of YOLOv7 for object detection and ArUco markers for size measurement can be useful in computer vision systems for a variety of applications, particularly when simultaneously performing both object detection and precise size measurement. There are several scenarios in which this approach is valuable in several scenarios. In agriculture, this approach can be used to count and measure fruit or crops in trees or fields. This aids yield estimation and resource planning. In construction and architecture, it aids in monitoring the dimensions of building components, ensuring that they meet design specifications. Combining object detection with precise size measurement is essential for augmented reality (AR) applications in which virtual objects must interact realistically with the physical world. In scientific research, this method can be used to measure the objects of interest with high precision, which is crucial for experiments and studies. When inspecting infrastructure, such as pipelines or bridges, This approach can help detect and measure defects or anomalies accurately when inspecting infrastructure such as pipelines or bridges. Retailers can benefit from this method by tracking and measuring items on the store shelves. This helps to optimize the inventory levels and ensure that the products are correctly placed [30]. Medical devices with integrated cameras can benefit from this approach for calibration and measurement. ArUco markers provide reference points for size measurements. This approach can be used to detect and measure components or products in a manufacturing environment. YOLOv7 identifies objects, whereas the ArUco markers provide precise reference sizes for quality control. Retail analytics systems can use this method to track and measure customer interaction with products on store shelves. This provides valuable insight into the popularity and placement of products. Robots equipped with cameras can use this method to detect objects in their surroundings and accurately measure their size. This is useful for tasks, such as picking, placing, and sorting objects. This approach can be used to track and measure the animal, plant, and environmental characteristics in wildlife conservation and environmental studies. The key advantage of this method is that it provides both detection and measurement capabilities within a single computer vision pipeline. This allows for the accurate and real-time measurement of objects in various domains, which can lead to improved efficiency, better decision-making, and enhanced automation in a wide range of applications.

ArUco markers are suitable for high-precision size measurements in controlled environments, whereas YOLOv7 excels in real-time and markerless object detection across various dynamic and uncontrolled domains. The choice between these two methods depends on the specific requirements and constraints of their application.

3) OBSERVATIONS

The researcher took live images from an orchard with fruits on a tree, applied this model to those images, and obtained very good size accuracy. Aruco markers were used on trees for fruit detection at a time. To obtain the weight [2] of the fruit using computer vision, the researcher expected to first obtain the fruit size in the form of height and width of the fruit in two directions. A single-stage fast and accurate detection algorithm named YOLOv7 was used. In this manner, the fruit is detected in the bounding box format; therefore, the researcher decided to obtain the fruit size in a bounding box format. To obtain the size in an h×w format, the researcher focused on the aruco marker, which is an image-processing artificial marker that provides the size in the form of, as expected by the researcher. The researchers used samples for fruit size estimation, as shown in Table 2.

TABLE 2. Various methods of fruit size finding concepts using aruco marker for on-tree mango.

Method	AM Size		Mango size			
	detect	Diff	W	H	Diff	Reason
Wrong AM [Fig14]	5.3×7.8	Yes	7.7	6.6	Yes	Marker wrongly pasted
AM [Fig15]	4.9×4.8	±0.2	NA	NA	Yes	Background also detected
AM+BS [Fig16]	5.1×5.1	±0.1	1.9	2.3	Only one fruit detected	Background removed
SS [Fig17]	5.1×5.1	±0.1	m1: 3.8 m2: 3.8 m3: 3.8 m4: 3.8	3.0 2.9 3.0 3.0	±0.1 at marker, and detected all the fruits with size.	Four fruits detected and predicted its size, because only fruits were visible

AM Size: Aruco Marker Size; BS: Background Subtraction; SS: Semantic Segmentation; Diff: Difference; W: Width; H: Height.

4) REQUIREMENT TO DETECT ONLY MANGO ON TREES

There are more than 1000 varieties of mangoes, and every mango is different in shape and color to predict all different types of mangoes with one mango-type dataset. The researcher used only one type of mango: Banganapalle. Problems faced while implementing the step-by-step procedure while using it in real time include the following: using the aruco marker and the image shown in Figure 14, we developed a method for size estimation.

5) COMBINED YOLOV7 AND ARUCO MARKER WITHOUT SEMANTIC SEGMENTATION FOR SIZE ESTIMATION

After obtaining a simple image-based mango fruit size, the researcher planned to determine the size of the on-tree mango fruit using YOLOv7 and an aruco marker for tree mango

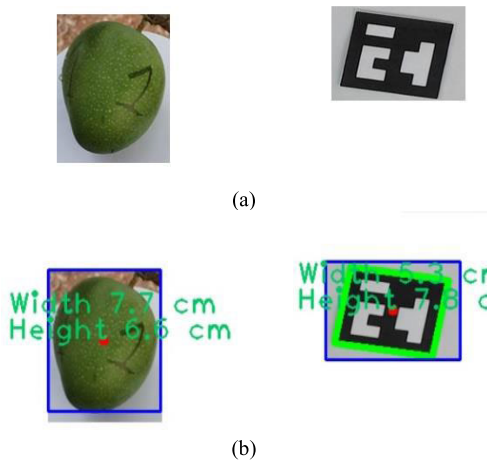


FIGURE 14. Fruit size estimation using ArUco marker, (a) An image with mango and aruco marker, (b) Resultant mango size as the width of the tree is 7.7 cm, and height is 6.6 cm.

fruit size estimation (Figure 15a), as shown in Figure 15b. The researcher considered the whole fruit, branch, and leaf, and obtained results that were not suitable for on-tree fruit size prediction. The researcher observed that with the help of an aruco marker, it detected all that was present in the image. To overcome this problem, the researcher performed background removal was performed as shown in Figure 15.

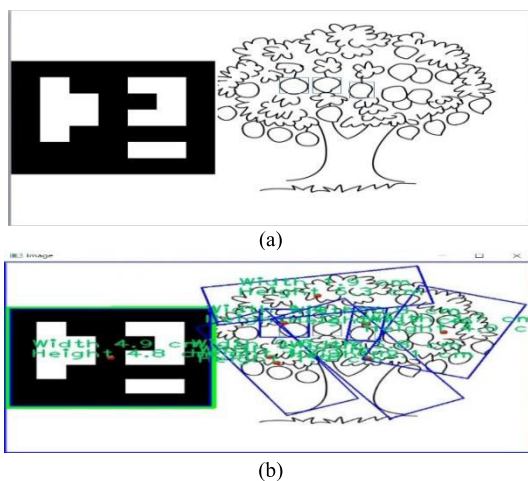


FIGURE 15. On tree Mango size estimation using aruco marker. (a) aruco marker with mango tree for mango size estimation as input image, (b) On tree size estimation of mango fruit with Aruco marker using image processing where it detected complete tree including fruits and leaves and branches.

After the use of YOLOv7 and the Aruco marker, various image-enhancement methods were developed, as shown in Figure 15, various image-enhancement methods have been developed. It was observed that background subtraction is important in this research to measure fruit size; therefore, the researcher focused on an image enhancement method to remove the background using background

removal/subtraction of tree mangoes. In this background subtraction concept, an input image with fruits was considered, and it was found that only one mango was detected in the foreground after removing and subtracting the background, as shown in Figure 16a. The researcher then performed size estimation, and the results are shown in Figure 16b. After doing this, the researcher observed the missing of all fruits that were present in the image, except for one fruit that was shown to us at the front end of the image, and found the size of the detected fruit, as shown in Figure 16b. To overcome this problem, researchers have focused on the semantic segmentation concept of input images.

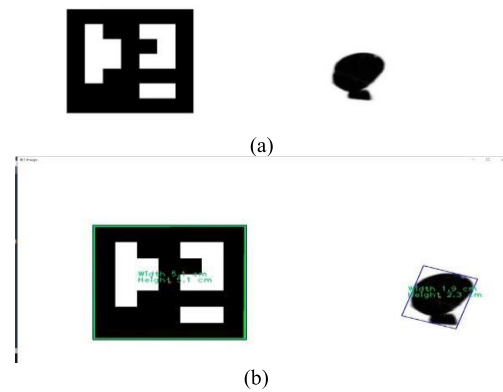


FIGURE 16. (a) An image enhancement method named background removal was used to get a better object view and for the size prediction. (b) Removed all in the scene except the front visible single mango for size estimation.

The mango fruit was detected using YOLOv7, and the aruco marker measured the size of the mango fruit on a tree, including the branches, leaves, and fruit. However, we did not want the size of the branches and leaves to be combined. We only needed the fruit size.

6) COMBINED YOLOV7, SEMANTIC SEGMENTATION, AND ARUCO MARKER FOR SIZE ESTIMATION

To overcome the problem shown in Figure 16, the researcher applied an image processing technique called the segmentation concept to the input image to separate the background of the image from the fruits in the image. The researcher focused on semantic segmentation, which supported the removal of all multiple backgrounds and gave us the expected foreground mangoes from the given input image (Figure 17a). Therefore, the researcher used semantic segmentation, removed the background, and used the background removed image as input for size estimation with the aruco marker to obtain the on-tree mango fruit size estimation, as shown in Figure 17b.

B. FUTURE WORK

Weight prediction of on-tree mango fruit using an artificial marker and QR-code, where researchers plan to store the details of the tree and fruit using different measures. Location details of the tree location and the orchard? What are the altitude and latitude of the tree? The number of trees, number

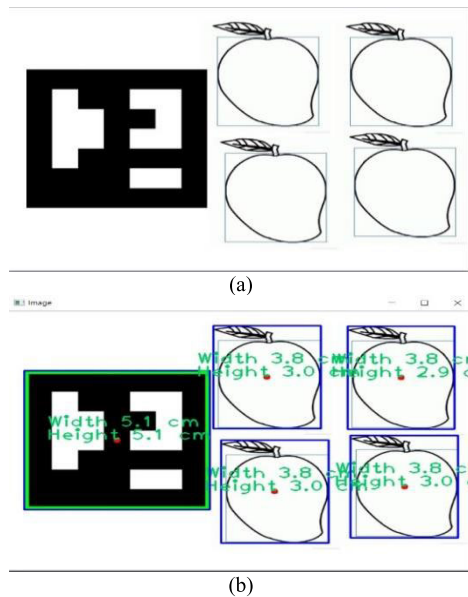


FIGURE 17. On tree multiple mango fruit size estimation at multiple background removal, (a) after semantic segmentation of background removed image, (b) Detected multiple mangos and Aruco marker image with size estimation.

of fruits on the tree, and total weight of the fruits on the required tree will be stored in a particular QR code for future reference to predict the weight. csv, which was manually measured using the height and width of the fruit to measure the fruit weight in grams, as shown in Figure 18. In today’s information communication systems, providing security to the data is very important, and QR codes can provide this security because of their high capacity; here, the researcher can use secure QR code technology for data security [1].

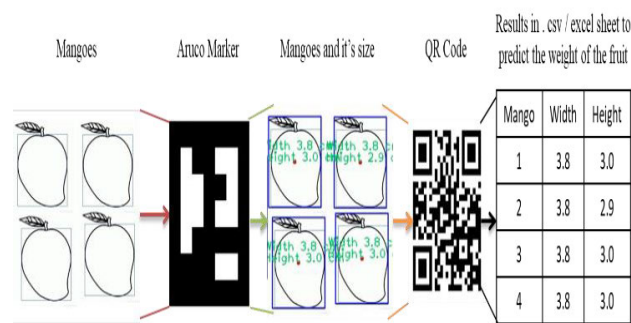


FIGURE 18. Future work to predict the weight of the fruit using an artificial marker and QR-code with deep learning.

VI. CONCLUSION

With the help of mango size estimation, it is possible to obtain the fruit weight using computer vision. Polygon-based object size, line-based object size, dotted-based object size with a fixed camera, and moving surface-based object size prediction were used; however, the researcher expected an object size in the bounding box dependent because with this

box type of mango, the size would give us the height and width of the mango fruit. If we are ready with the height and width of the mango fruit, it is possible to obtain the mango weight in grams to predict the yield. In this size estimation, the Aruco marker is visible only at the corner of the former but not at the customer or someone else. The Aruco marker is an augmented reality-based marker that is used as the base reference for visually sizing the fruit. In the tree, Banganapalle mango fruit detection was performed using the YOLOv7 algorithm, which was used for image background removal, and the multi-object foreground mango fruit was detected. and Multiple backgrounds, such as leaves and branches, were removed from the tree and an augmented reality-based artificial marker of the image processing technique was used for fruit size prediction in the length and width of the bounding box format. Two possible size measurement techniques were used. Overlapping and non-overlapping fruit size measurements. Where, the researcher can apply this model to get the size of the fruit for better yield prediction and apply this model on it and got good results such as 84% of accuracy, 91% precision, and 89% recall at overlapping mango fruit on tree images. For non-overlapping mango fruit, the average accuracy of the width and height prediction is 96.7%, and it is too good for non-occluded fruit on tree size measurement.

REFERENCES

- [1] M. S. Ahamed and H. A. Mustafa, “A secure QR code system for sharing personal confidential information,” in *Proc. Int. Conf. Comput., Commun., Mater. Electron. Eng.*, Jul. 2019, pp. 1–4, doi: 10.1109/IC4ME247184.2019.9036521.
- [2] H. A. G. Al-Kaf and K. S. Chia, “The size and weight prediction for intact pineapples using a low cost vision system,” in *Proc. Zooming Innov. Consum. Technol. Conf. (ZINC)*, May 2020, pp. 146–150, doi: 10.1109/ZINC50678.2020.9161770.
- [3] M. H. Amaral and K. B. Walsh, “In-orchard sizing of mango fruit: 2. Forward estimation of size at harvest,” *Horticulturae*, vol. 9, no. 1, p. 54, Jan. 2023, doi: 10.3390/horticulturae9010054.
- [4] M. Arzt, J. Deschamps, C. Schmied, T. Pietzsch, D. Schmidt, P. Tomancak, R. Haase, and F. Jug, “LABKIT: Labeling and segmentation toolkit for big image data,” *Frontiers Comput. Sci.*, vol. 4, p. 10, Feb. 2022, doi: 10.3389/fcomp.2022.777728.
- [5] D. Avola, L. Cinque, G. L. Foresti, C. Mercuri, and D. Pannone, “A practical framework for the development of augmented reality applications by using ArUco markers,” in *Proc. ICPRAM* Feb. 2016, pp. 645–654, doi: 10.5220/0005755806450654.
- [6] H. Caesar, J. Uijlings, and V. Ferrari, “Region-based semantic segmentation with end-to-end training,” *Computer Vision—ECCV 2016*. Cham, Switzerland: Springer, 2016, doi: 10.1007/978-3-319-46448-0_23.
- [7] Z. Cai and N. Vasconcelos, “Cascade R-CNN: High quality object detection and instance segmentation,” *IEEE Trans. Pattern Anal. Mach. Intell.*, vol. 43, no. 5, pp. 1483–1498, May 2021, doi: 10.1109/TPAMI.2019.2956516.
- [8] J. Čejka, F. Bruno, D. Skarlatos, and F. Liarokapis, “Detecting square markers in underwater environments,” *Remote Sens.*, vol. 11, no. 4, p. 459, Feb. 2019, doi: 10.3390/rs11040459.
- [9] M. T. Cazzolato, J. S. Ramos, L. S. Rodrigues, L. C. Scabora, D. Y. T. Chino, A. E. S. Jorge, P. M. de Azevedo-Marques, C. Traina, and A. J. M. Traina, “The UTrack framework for segmenting and measuring dermatological ulcers through telemedicine,” *Comput. Biol. Med.*, vol. 134, Jul. 2021, Art. no. 104489, doi: 10.1016/j.combiomed.2021.104489.
- [10] S. Dhameliya, J. Kakadiya, and R. Savant, “Volume estimation of mango,” *Int. J. Comput. Appl.*, vol. 143, no. 12, pp. 11–16, Jun. 2016, doi: 10.5120/ijca2016910056.

- [11] H. Ding, H. Zhang, C. Liu, and X. Jiang, "Deep interactive image matting with feature propagation," *IEEE Trans. Image Process.*, vol. 31, pp. 2421–2432, 2022, doi: [10.1109/TIP.2022.3155958](https://doi.org/10.1109/TIP.2022.3155958).
- [12] S. Garrido-Jurado, R. Muñoz-Salinas, F. J. Madrid-Cuevas, and M. J. Marín-Jiménez, "Automatic generation and detection of highly reliable fiducial markers under occlusion," *Pattern Recognit.*, vol. 47, no. 6, pp. 2280–2292, Jun. 2014, doi: [10.1016/j.patcog.2014.01.005](https://doi.org/10.1016/j.patcog.2014.01.005).
- [13] J. Gené-Mola, M. Ferrer-Ferrer, E. Gregorio, P. M. Blok, J. Hemming, J.-R. Morros, J. R. Rosell-Polo, V. Vilaplana, and J. Ruiz-Hidalgo, "Looking behind occlusions: A study on amodal segmentation for robust on-tree apple fruit size estimation," *Comput. Electron. Agricult.*, vol. 209, Jun. 2023, Art. no. 107854, doi: [10.1016/j.compag.2023.107854](https://doi.org/10.1016/j.compag.2023.107854).
- [14] M. A. Ghazi, L. Ding, A. H. Fagg, T. H. A. Kolobe, and D. P. Miller, "Vision-based motion capture system for tracking crawling motions of infants," in *Proc. IEEE Int. Conf. Mechatronics Autom. (ICMA)*, Aug. 2017, pp. 1549–1555, doi: [10.1109/ICMA.2017.8016047](https://doi.org/10.1109/ICMA.2017.8016047).
- [15] Y. Guo, Y. Liu, T. Georgiou, and M. S. Lew, "A review of semantic segmentation using deep neural networks," *Int. J. Multimedia Inf. Retr.*, vol. 7, no. 2, pp. 87–93, Jun. 2018, doi: [10.1007/s13735-017-0141-z](https://doi.org/10.1007/s13735-017-0141-z).
- [16] S. Hao, Y. Zhou, and Y. Guo, "A brief survey on semantic segmentation with deep learning," *Neurocomputing*, vol. 406, pp. 302–321, Sep. 2020, doi: [10.1016/j.neucom.2019.11.118](https://doi.org/10.1016/j.neucom.2019.11.118).
- [17] M. Kalaitzakis, B. Cain, S. Carroll, A. Ambrosi, C. Whitehead, and N. Vitzilaios, "Fiducial markers for pose estimation: Overview, applications and experimental comparison of the ARTag, AprilTag, ArUco and STag markers," *J. Intell. Robot. Syst.*, vol. 101, no. 4, Apr. 2021, doi: [10.1007/s10846-020-01307-9](https://doi.org/10.1007/s10846-020-01307-9).
- [18] D. Khan, S. Ullah, D.-M. Yan, I. Rabbi, P. Richard, T. Hoang, M. Billinghurst, and X. Zhang, "Robust tracking through the design of high quality fiducial markers: An optimization tool for ARToolKit," *IEEE Access*, vol. 6, pp. 22421–22433, 2018, doi: [10.1109/ACCESS.2018.2801028](https://doi.org/10.1109/ACCESS.2018.2801028).
- [19] A. Kirillov, K. He, R. Girshick, C. Rother, and P. Dollár, "Panoptic segmentation," in *Proc. IEEE/CVF Conf. Comput. Vis. Pattern Recognit. (CVPR)*, Jun. 2019, pp. 9396–9405, doi: [10.1109/CVPR.2019.00963](https://doi.org/10.1109/CVPR.2019.00963).
- [20] J. Lazarow, K. Lee, K. Shi, and Z. Tu, "Learning instance occlusion for panoptic segmentation," in *Proc. IEEE/CVF Conf. Comput. Vis. Pattern Recognit. (CVPR)*, Jun. 2020, pp. 10717–10726, doi: [10.1109/CVPR42600.2020.01073](https://doi.org/10.1109/CVPR42600.2020.01073).
- [21] Y. Liu, X. Xu, Q. Yu, Q. Pu, J. Gao, X. Wang, Z. Wang, H. Wang, S. Xu, A. Rodic, and P. B. Petrovic, "Simultaneous localization and mapping of unmanned vehicles under dynamic environments with YOLOv7," in *Proc. IEEE Int. Conf. Robot. Biomimetics (ROBIO)*, Dec. 2022, pp. 898–903, doi: [10.1109/ROBIO55434.2022.10011889](https://doi.org/10.1109/ROBIO55434.2022.10011889).
- [22] S. Minaee, Y. Boykov, F. Porikli, A. Plaza, N. Kehtarnavaz, and D. Terzopoulos, "Image segmentation using deep learning: A survey," *IEEE Trans. Pattern Anal. Mach. Intell.*, vol. 44, no. 7, pp. 3523–3542, Jul. 2022, doi: [10.1109/TPAMI.2021.3059968](https://doi.org/10.1109/TPAMI.2021.3059968).
- [23] O. Mirbod, D. Choi, P. H. Heinemann, R. P. Marini, and L. He, "On-tree apple fruit size estimation using stereo vision with deep learning-based occlusion handling," *Biosyst. Eng.*, vol. 226, pp. 27–42, Feb. 2023, doi: [10.1016/j.biosystemseng.2022.12.008](https://doi.org/10.1016/j.biosystemseng.2022.12.008).
- [24] O. Mirbod, L. Yoder, and S. Nuske, "Automated measurement of berry size in images this work is supported in part by the national grape and wine initiative and the US department of agriculture under grant number 20126702119958," *IFAC-PapersOnLine*, vol. 49, no. 16, pp. 79–84, 2016, doi: [10.1016/j.ifacol.2016.10.015](https://doi.org/10.1016/j.ifacol.2016.10.015).
- [25] A. Moffat, "Huffman coding," *ACM Comput. Surv.*, vol. 52, no. 4, pp. 1–35, Jul. 2020, doi: [10.1145/3342555](https://doi.org/10.1145/3342555).
- [26] P. Risholm, P. Ø. Ivarsen, K. H. Haugholt, and A. Mohammed, "Underwater marker-based pose-estimation with associated uncertainty," in *Proc. IEEE/CVF Int. Conf. Comput. Vis. Workshops (ICCVW)*, Oct. 2021, pp. 3706–3714, doi: [10.1109/ICCVW54120.2021.00414](https://doi.org/10.1109/ICCVW54120.2021.00414).
- [27] J. Schindelin, I. Arganda-Carreras, E. Frise, V. Kaynig, M. Longair, T. Pietzsch, S. Preibisch, C. Rueden, S. Saalfeld, B. Schmid, J.-Y. Tinevez, D. J. White, V. Hartenstein, K. Eliceiri, P. Tomancak, and A. Cardona, "Fiji: An open-source platform for biological-image analysis," *Nature Methods*, vol. 9, no. 7, pp. 676–682, Jul. 2012, doi: [10.1038/nmeth.2019](https://doi.org/10.1038/nmeth.2019).
- [28] E. Shelhamer, J. Long, and T. Darrell, "Fully convolutional networks for semantic segmentation," *IEEE Trans. Pattern Anal. Mach. Intell.*, vol. 39, no. 4, pp. 640–651, Apr. 2017, doi: [10.1109/TPAMI.2016.2572683](https://doi.org/10.1109/TPAMI.2016.2572683).
- [29] Z. Siki and B. Takács, "Automatic recognition of ArUco codes in land surveying tasks," *Baltic J. Mod. Comput.*, vol. 9, no. 1, pp. 115–125, 2021, doi: [10.22364/bjmc.2021.9.1.06](https://doi.org/10.22364/bjmc.2021.9.1.06).
- [30] M. Stenmark, E. Omerbašić, M. Magnusson, V. Andersson, M. Abrahamsson, and P.-K. Tran, "Vision-based tracking of surgical motion during live open-heart surgery," *J. Surgical Res.*, vol. 271, pp. 106–116, Mar. 2022, doi: [10.1016/j.jss.2021.10.025](https://doi.org/10.1016/j.jss.2021.10.025).
- [31] T. Tocci, L. Capponi, and G. Rossi, "ArUco marker-based displacement measurement technique: Uncertainty analysis," *Eng. Res. Exp.*, vol. 3, no. 3, Sep. 2021, Art. no. 035032, doi: [10.1088/2631-8695/ac1fc7](https://doi.org/10.1088/2631-8695/ac1fc7).
- [32] L. Tzatalin. (2021). *Git Code*. Accessed: Apr. 2020. [Online]. Available: <https://github.com/tzatalin/labelimg>
- [33] C.-Y. Wang, A. Bochkovskiy, and H.-Y.-M. Liao, "YOLOv7: Trainable bag-of-freebies sets new state-of-the-art for real-time object detectors," in *Proc. IEEE/CVF Conf. Comput. Vis. Pattern Recognit. (CVPR)*, Jun. 2023, pp. 7464–7475.
- [34] Z. Wang, K. Walsh, and B. Verma, "On-tree mango fruit size estimation using RGB-D images," *Sensors*, vol. 17, no. 12, p. 2738, Nov. 2017, doi: [10.3390/s17122738](https://doi.org/10.3390/s17122738).
- [35] Y. Wei, Q. Tian, J. Guo, W. Huang, and J. Cao, "Multi-vehicle detection algorithm through combining Harr and HOG features," *Math. Comput. Simul.*, vol. 155, pp. 130–145, Jan. 2019, doi: [10.1016/j.matcom.2017.12.011](https://doi.org/10.1016/j.matcom.2017.12.011).
- [36] H. Yu, Z. Yang, L. Tan, Y. Wang, W. Sun, M. Sun, and Y. Tang, "Methods and datasets on semantic segmentation: A review," *Neurocomputing*, vol. 304, pp. 82–103, Aug. 2018, doi: [10.1016/j.neucom.2018.03.037](https://doi.org/10.1016/j.neucom.2018.03.037).
- [37] J. Yu, W. Jiang, Z. Luo, and L. Yang, "Application of a vision-based single target on robot positioning system," *Sensors*, vol. 21, no. 5, p. 1829, Mar. 2021, doi: [10.3390/s21051829](https://doi.org/10.3390/s21051829).



DEVENDER NAYAK NENAVATH was born in Vikarabad, Telangana, India, in 1988. He received the B.Tech. degree in information technology and the M.Tech. degree in computer science and engineering from Jawaharlal Nehru Technological University, Hyderabad, in 2012 and 2014, respectively, and the Ph.D. degree from the Vellore Institute of Technology University, Vellore, Tamil Nadu, India. His research interests include cloud computing and artificial intelligence.



BOOMINATHAN PERUMAL (Member, IEEE) was born in Virudhachalam, Tamil Nadu, India, in 1981. He received the B.E. degree in computer science and engineering from Bharathidasan University, in 2003, the M.E. degree in computer science and engineering from Anna University, in 2005, and the Ph.D. degree in computer science and engineering from the Vellore Institute of Technology University, Vellore, India, in 2017.

From 2005 to 2010, he was a Lecturer in different colleges. In 2010, he joined the Vellore Institute of Technology as an Assistant Professor, where he is currently a Senior Associate Professor. He is the coauthor of five books and published more than 20 articles. His research interests include cloud computing, artificial intelligence, knowledge graphs, and blockchain technology.

Dr. Perumal holds a lifetime professional membership with the Computer Society of India (CSI).

• • •